

# The Impact of High-Rise Building Shapes on Wind Flow Characteristics and Energy Potential

Ehsan Mokhtari, Amir Hossein Jafari, Roslina Sharif, Wan Srihani wan Mohamed



**Abstract.** In recent years, wind energy has become a potential source of low carbon energy. The shape of a building is a significant factor in aerodynamics, providing an opportunity for wind power control and wind energy proliferation. This research project aims to study the design of high-rise buildings and investigate how wind affects energy absorption by developing an aerodynamic optimization procedure (AOP) and using Computational Fluid Dynamics (CFD) in COMSOL Multiphysics. This study aimed to optimize the building shape for wind energy exploitation. Optimizing the building shape in the early stages of design enables the control of wind-induced loads and responses and reduces the energy demand in high-rise buildings, where resource consumption is higher than that in low-height buildings. This study used a three-dimensional CFD simulation of wind loading on tall buildings to optimize the building shape. This research will provide valuable insights for architects, engineers, and building developers to design and optimize high-rise buildings for wind energy exploitation, reduce the carbon footprint, and improve the energy efficiency of buildings.

**Keywords:** Aerodynamics, Computational Fluid Dynamics (CFD), High-rise Buildings, Shape Modification, Wind Energy, Wind Velocity

## I. INTRODUCTION

Each urban area has its own roughness and typical wind characteristics, as urban roughness increases with height and wind speed [1][26][27]. This demonstrates that the urban environment has the potential to conserve wind energy and provide energy efficiency, which in turn can reduce energy loss, air pollutants, and carbon emissions [2]. The ultimate impact of shrinking carbon emissions will bring economic growth to urban areas of big cities. Regarding the reduction of energy consumption, Directive 2010/31/EU is adopting an approach at an early stage in the design of buildings to take advantage of renewable energy facilities, such as wind power.

In a similar study, the operational efficiency of a vertical-axis wind turbine was evaluated under environmental turbulence conditions. Their results showed that vertical wind had a clear effect on the power output when horizontal wind speeds were within a certain range. These results can be employed as a reference for selecting aerodynamic properties, output efficiency, CFD simulations and vertical wind turbine position. Omid Esmaili claims that the combination of building shape, height, and composition may cause human discomfort that cannot be accommodated by inducing strong wind currents near the ground.

In his treatise, a popular situation of urban planning was covered, which amplified the ground wind speed over a tall building of 56-story. Concerns about the quality of urban public spaces were raised by Sigrid Reiter, who focused on the progression of CFD and computational fluid dynamics. Providing a simple graphical tool, he developed a new methodology for quantifying wind speeds around buildings. The study results can serve as a simple design tool for architects and urban planners to consider wind in the design of the built environment.

In this study, the main parameters of the atmospheric boundary layer were considered to determine whether the upstream wind flow was sufficiently generated in the numerical simulations. Computational Wind Tunnel tests were conducted and the influence of wind loads on the design of low-to mid-rise buildings was demonstrated. The survey results showed that wind pressure was much greater than the other factors in the CWT tests. For the efficient harvesting of wind energy [3], proposed opening strategies for a double-skin façade system.

Effect of twisted wind flows on pedestrian-level wind fields in an urban environment. Highlighted four twisted wind flows of different magnitudes and employed yaw angle directions to find wind speed variations resulting from the characteristics of twisted wind profiles at the pedestrian level. Using a two-step approach [4], analyzed the impact of wind on distant sound propagation over various generic urban sections in downward atmospheric refraction. They first simulated the wind field using computational fluid dynamics, and then adopted the mean wind field approach in computational acoustics.

It was discovered that common criteria for pedestrian comfort led to varying conclusions, conditional on accessibility to data of high spatiotemporal resolution. The current study is a step forward to the latest advances in wind power exploitation, analyzing different forms of tall buildings of the same height in terms of wind power absorption.

Manuscript received on 01 November 2023 | Revised Manuscript received on 12 November 2023 | Manuscript Accepted on 15 November 2023 | Manuscript published on 30 March 2024.

\* Correspondence Author (s)

Ehsan Mokhtari, Department of Design and Architecture, Faculty of Design and Architecture, Universiti Putra Malaysia, UPM Serdang, Malaysia  
Amir Hossein Jafari, Department of Civil Engineering, Islamic Azad University- Lahijan, Iran. ORCID ID: [0000-0002-4415-0946](https://orcid.org/0000-0002-4415-0946)

Roslina Sharif, Department of Design and Architecture, Faculty of Design and Architecture, Universiti Putra Malaysia, UPM Serdang, Malaysia. ORCID ID: [0000-0001-8329-5606](https://orcid.org/0000-0001-8329-5606)

Wan Srihani wan Mohamed\*, Department of Design and Architecture, Faculty of Design and Architecture, Universiti Putra Malaysia, UPM Serdang, Malaysia. E-mail: [rsrihani@upm.edu.my](mailto:rsrihani@upm.edu.my), ORCID ID: [0009-0009-5460-1470](https://orcid.org/0009-0009-5460-1470)

© The Authors. Published by Lattice Science Publication (LSP). This is an open access article under the CC-BY-NC-ND license (<http://creativecommons.org/licenses/by-nc-nd/4.0/>)

## II. EXPERIMENTAL METHODOLOGY

### A. Study Data

The general features of the climate in Malaysia include high humidity, uniform temperature, copious rainfall, and light winds. As Malaysia has shown low readiness for the use of solar radiation power, wind absorption in high-rise buildings was selected as a way to preserve energy. Wind speed data were collected from field measurements of four case studies that represent four types of high-rise buildings in Penang, Malaysia. This research was carried out on the top of case buildings, where the wind location had a chance to be evaluated for the possibility of wind turbines, and the wind condition was less affected by the surface roughness. The participants of this research were four high-rise buildings, one known as Komtar Tower factually located in Penang, Malaysia, and the other three were hypothetical geometries diverse in roof plans with both curved-edge and straight-edge types. The Komtar Tower is the eleventh tallest in Malaysia and the tallest skyscraper in the state. Fig. 1. Shows the selected geometries of the four high-rise buildings considered in this study.

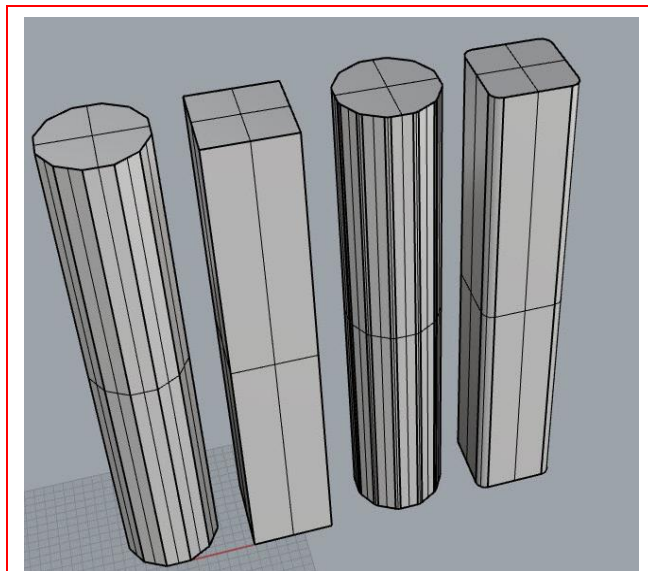


Fig. 1: The Selected Types of High-Rise Building

### B. Computational Fluid Dynamics (CFD)

Computational fluid dynamics (CFD) is a science that, with the help of digital computers, produces quantitative predictions of fluid flow phenomena based on the conservation laws (conservation of mass, momentum, and energy) governing fluid motion. It has expanded in importance and accuracy; however, its forecasts are inaccurate. Moreover, mathematical models and numerical algorithms are used to simulate the behavior of fluids such as air. CFD can be used to analyze the airflow around buildings and estimate the wind velocity on building surfaces.

### C. COMSOL Multiphysics

This research was based on two types of data: local wind data and wind data observed from field measurements. Table 1 illustrates the effective parameters used in COMSOL simulations. In this table, V1 accounts for the speed of wind at H1 height, H1 refers to the height of V1, H2 is the height of the gradient, V2 is the wind speed at height H2, and Z0 is

the roughness length (towns, villages, agricultural land with many or high hedges, forests, and very rough and uneven terrain). The temperature for all the simulations was taken at a constant number of 293.15 K.

Table-1: The Input Parameters for Wind Speed Analysis in Comsol

V1 (m/s)	H1 (m)	H2 (m)	Z0 (m)	V2 (m/s)
2.78	10	300	0.4	5.7

We adopted the  $k-\epsilon$  turbulence model for our wind tunnel simulation in CFD and the turbulence velocity time scale, which includes two additional transport equations and two dependent variables: the turbulent kinetic energy,  $k$ , and turbulent dissipation rate,  $\epsilon$ . the turbulent viscosity is modeled as follows:

$$(Eq.1)$$

$\mu_T = \rho C_\mu \frac{k^2}{\epsilon}$  where  $C_\mu$  is a model constant. The transport equation for  $k$  reads: (Eq. 2)  $\rho \frac{\partial k}{\partial t} + \rho u \cdot \nabla k = \nabla \cdot ((\mu + \frac{\mu_T}{\sigma_k}) \nabla k) + P_k - \rho \epsilon$  where the production term is: (Eq. 3)  $P_k = \mu_T (\nabla u : (\nabla u + \nabla u^T) - \frac{2}{3} (\nabla \cdot u)^2) - \frac{2}{3} \rho k \nabla \cdot u$

The transport equation for  $\epsilon$  reads: (Eq. 4)  $\rho \frac{\partial \epsilon}{\partial t} + \rho u \cdot \nabla \epsilon = \nabla \cdot ((\mu + \frac{\mu_T}{\sigma_\epsilon}) \nabla \epsilon) + C_{\epsilon 1} \frac{\epsilon}{k} P_k - C_{\epsilon 2} \rho \frac{\epsilon^2}{k}$

The model constants in Equations 1, 2, and 3 were determined from the experimental data and values proposed by Versteeg and Malalasekera [5], as listed in Table 2. This turbulence model was applied in all simulations in the current study.

Table-2: Model Constants

CONSTANT	$C_\mu$	$C_{\epsilon 1}$	$C_{\epsilon 2}$	$\sigma_k$	$\sigma_\epsilon$
VALUE	0.09	1.44	1.92	1.00	1.3

Table Nomenclature:  $\mu$  =The fluid's dynamic viscosity (SI unit:  $\text{kg}/(\text{m}\cdot\text{s})$ ),  $\mu_T$  = Turbulent viscosity (SI unit:  $\text{kg}/(\text{m}\cdot\text{s})$ ),  $u$ = The velocity field (SI unit:  $\text{m}/\text{s}$ ),  $\rho$  = The density of the fluid (SI unit:  $\text{kg}/\text{m}^3$ ),  $k$ Turbulent kinetic energy (SI unit:  $\text{m}^2/\text{s}^2$ ),  $\epsilon$ =Turbulent dissipation rate (SI unit:  $\text{m}^2/\text{s}^3$ )

Because air is defined as the material, we applied the incompressible flow formulation to gases at low velocities in the case of constant  $\rho$  in COMSOL. Based on the continuity equation for incompressible fluids, Reynolds-averaged Navier–Stokes equations (RANS) were used as the turbulence model type. Developed by Osborne Reynolds [6], RANS equations are connected with Reynolds decomposition, in which an instantaneous quantity is broken into fluctuating and time-averaged quantities to represent turbulent flows [7]. The accuracy of the simulations also depends on the type of meshing and the size of the wind tunnel. In this research, meshing was performed with free tetrahedral meshed cells with five boundary layers considered on the ground walls and a no-slip boundary condition assumed on the ground surface, Fig. 2.

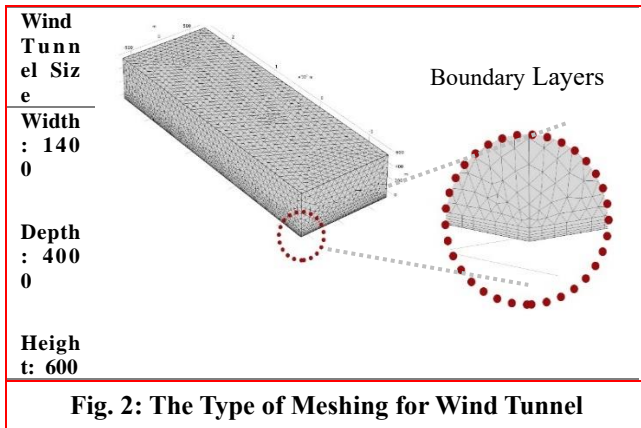


Fig. 2: The Type of Meshing for Wind Tunnel

**D. Reynolds Averaged Navier-Stokes Equations**

Using the time-averaged equations of motion for wind flow and the continuity equation for incompressible fluid flow, the basic equations for the mean values of turbulent flow are as follows: The wind flow field was defined using mean values. The wind flow field was then defined using these mean values, Fig. 3.

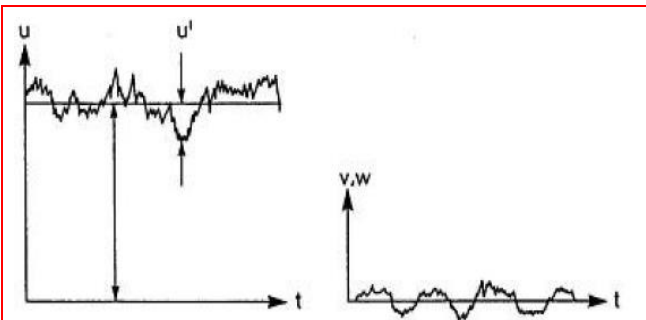


Fig. 3: Turbulent Velocity Fluctuation in Pipe Flow as A Function of Time [8]

The momentary velocity is defined by  $u$ , the time-averaged value by  $\bar{u}$ , and the fluctuating velocity by the letter  $u'$ . With this mathematical definition, the decomposition is written as Eq. 4-1:  $u = \bar{u} + u', v = \bar{v} + v', w = \bar{w} + w', p = \bar{p} + p'$

Similarly, for density and temperature, we obtained Eq. 4-2:  $\rho = \bar{\rho} + \rho', T = \bar{T} + T'$

which are considered constant in the following equation.

The chosen averaging method took the mean values at a fixed place in space, and the time span was sufficiently large to be independent of the mean values.

$$\text{Eq. 4-3: } \bar{u} = \frac{1}{\Delta t} \int_{t_0}^{t_0+\Delta t} u dt$$

The time-averaged fluctuating values were described as zero:

$$\text{Eq. 4-4: } \overline{u'} = 0, \overline{v'} = 0, \overline{w'} = 0, \overline{p'} = 0$$

The continuity equation was then averaged. The expressions were substituted for the velocities from Eq.4-1 into the continuity equation to obtain

$$\text{Eq. 4-5: } \frac{\partial \bar{u}}{\partial x} + \frac{\partial \bar{u}'}{\partial x} + \frac{\partial \bar{v}}{\partial y} + \frac{\partial \bar{v}'}{\partial y} + \frac{\partial \bar{w}}{\partial z} + \frac{\partial \bar{w}'}{\partial z} = 0$$

The time average of the last equation is obtained as:

$$\text{Eq.4-6:}$$

$$\frac{\partial \bar{u}}{\partial x} + \frac{\partial \bar{u}'}{\partial x} + \frac{\partial \bar{v}}{\partial y} + \frac{\partial \bar{v}'}{\partial y} + \frac{\partial \bar{w}}{\partial z} + \frac{\partial \bar{w}'}{\partial z} = 0$$

Before the transformation and reduction of Eq. 4-6, the rules

for time-averaging are summarized as follows:

$$\text{Eq. 4-7: } \frac{\partial \bar{u}}{\partial x} = \frac{1}{\Delta t} \int_{t_0}^{t_0+\Delta t} \frac{\partial u}{\partial x} dt = \frac{\partial}{\partial x} \frac{1}{\Delta t} \int_{t_0}^{t_0+\Delta t} u dt = \frac{\partial \bar{u}}{\partial x}$$

$$\text{Eq. 4-8: } \frac{\partial \bar{u}'}{\partial x} = \frac{1}{\Delta t} \int_{t_0}^{t_0+\Delta t} \frac{\partial u'}{\partial x} dt = \frac{\partial}{\partial x} \frac{1}{\Delta t} \int_{t_0}^{t_0+\Delta t} u' dt = 0$$

$$\text{Eq. 4-9: } \overline{\bar{f}} = \bar{f}, \overline{\bar{f} + \bar{g}} = \bar{f} + \bar{g}, \overline{\bar{f} \cdot \bar{g}} = \bar{f} \cdot \bar{g}, \frac{\partial \bar{f}}{\partial s} = \frac{\partial f}{\partial s}, \overline{\int f ds} = \int \bar{f} ds$$

$$\text{But } \overline{\bar{f} \cdot \bar{g}} \neq \bar{f} \cdot \bar{g}$$

According to these rules, the averaged derivatives of the fluctuations were also zero. Thus, the time-averaged continuity equation was obtained:

$$\text{Eq. 4-10: } \frac{\partial \bar{u}}{\partial x} + \frac{\partial \bar{v}}{\partial y} + \frac{\partial \bar{w}}{\partial z} = 0$$

Now, the NS equations are time averaged. Averaging was exemplified for the x-component before a small transformation of the advection term:

$$\text{Eq. 4-11: } u \frac{\partial u}{\partial x} + v \frac{\partial u}{\partial y} + w \frac{\partial u}{\partial z} = \frac{\partial (u^2)}{\partial x} + \frac{\partial (uv)}{\partial y} + \frac{\partial (uw)}{\partial z} - \left( \frac{\partial u}{\partial x} + \frac{\partial v}{\partial y} + \frac{\partial w}{\partial z} \right) u = \frac{\partial (u^2)}{\partial x} + \frac{\partial (uv)}{\partial y} + \frac{\partial (uw)}{\partial z}$$

The expressions for the decomposition of the velocity values from Eq. 4-1 were then substituted into the transformed NS equation to obtain the time average:

$$\text{Eq.4-12: } \rho \left\{ \frac{\partial (\bar{u} + u')}{\partial t} + \frac{\partial (\bar{u} + u')^2}{\partial x} + \frac{\partial (\bar{u} + u')(\bar{v} + v')}{\partial y} + \frac{\partial (\bar{u} + u')(\bar{w} + w')}{\partial z} \right\} = F_x - \frac{\partial (\bar{p} + p')}{\partial x} + \mu \left( \frac{\partial^2 (\bar{u} + u')}{\partial x^2} + \frac{\partial^2 (\bar{u} + u')}{\partial y^2} + \frac{\partial^2 (\bar{u} + u')}{\partial z^2} \right)$$

The small transformations, including the repeated application of the product rule and advection term, resulted in the following time-averaged NS equations in all three directions:

$$\text{Eq. 4-13: } \rho \frac{D \bar{u}_i}{Dt} = F_i - \frac{\partial \bar{p}}{\partial x_i} + \mu \Delta \bar{u}_i - \rho \left( \frac{\partial \bar{u}'_i u'_j}{\partial x_j} \right)$$

The time-averaged fields were no longer overlined. For instance,  $u$  refers to the time-averaged velocity component along the x axis. The last two terms on the right-hand side of Eqs. 4-13 were noticed:

$$\text{Eq. 4-14: } \mu \Delta u_i - \rho \left( \frac{\partial \bar{u}'_i u'_j}{\partial x_j} \right) = \mu \frac{\partial}{\partial x_j} \left( \frac{\partial u_i}{\partial x_j} \right) - \rho \frac{\partial}{\partial x_j} (\overline{u'_i u'_j})$$

The expression in brackets above is the total shear stress.

$$\text{Eq. 4-15: } \tau_{ij} = \mu \frac{\partial u_i}{\partial x_j} - \rho \overline{u'_i u'_j}$$

Compared with the NS equation, it was added to the entire shear stress in addition to the viscous part. This term is derived from the time average as the dominant part of the entire shear stress. The term is called the Reynolds stress or turbulent shear stress, which expresses the Reynolds average. To complete the system of equations, the Reynolds stress was approximated in relation to the average flow velocity field and turbulent shear stress. The principle of the viscosity approach of Boussinesq [9], Reynolds equations, and the general time-averaged Navier–Stokes equation are formulated as follows:



# The Impact of High-Rise Building Shapes on Wind Flow Characteristics and Energy Potential

$$\text{Eq. 4-16: } \rho \left( \frac{D\bar{u}_i}{Dt} \right) = F_i - \frac{\partial \bar{p}}{\partial x_i} + \frac{\partial}{\partial x_j} \tau_{ij}$$

$$\text{With } \mu \frac{\partial u_i}{\partial x_j} - \rho \left( v_T \left( \frac{\partial u_i}{\partial x_j} + \frac{\partial u_j}{\partial x_i} \right) - \frac{2}{3} k \delta_{ij} \right)$$

## E. Validation Process

By changing the flow pattern around the building owing to aerodynamic modifications of the building shape, the wind response can be moderated compared to the original building shape. The wind tunnel test is the most popular method for evaluating the aerodynamic behavior of high-rise buildings. We successfully validated our model using airflow over an Ahmed body proposed by Ahmed, Ramm, and Faltn as a benchmark for aerodynamic simulation. A detailed measurement was performed in a wind tunnel for Reynolds number flows with flow visualization results, Fig. 4.

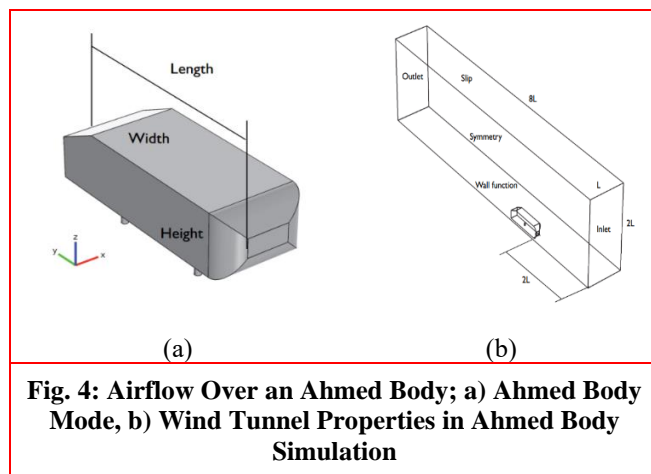


**Fig. 4: Airflow Over an Ahmed Body; a) Ahmed Body Mode, b) Wind Tunnel Properties in Ahmed Body Simulation**

## III. RESULTS

### A. Simulation Result

The 3D normal RANS equation is often applied to external flow problems around complex shapes and is solved using the k-epsilon turbulence model. The K-epsilon model finds solutions to two variables: turbulent kinetic energy and the rate of kinetic energy consumption. The nonlinear solver iteratively expands the equation to obtain sting. In this project, a CFD simulation was conducted and analyzed for four case studies located in the heart of a wind tunnel, and the results showed the effect of high-rise building geometry on aerodynamics. The other three models had approximately the same average speed, although the magnitude of the speed varied from tower to tower. Actual Models C, B, A, and D tended to intensify wind power. The effect of turbulence was observed at a maximum velocity of 7.21 for Model C with no potential velocity fluctuations Fig. 5.

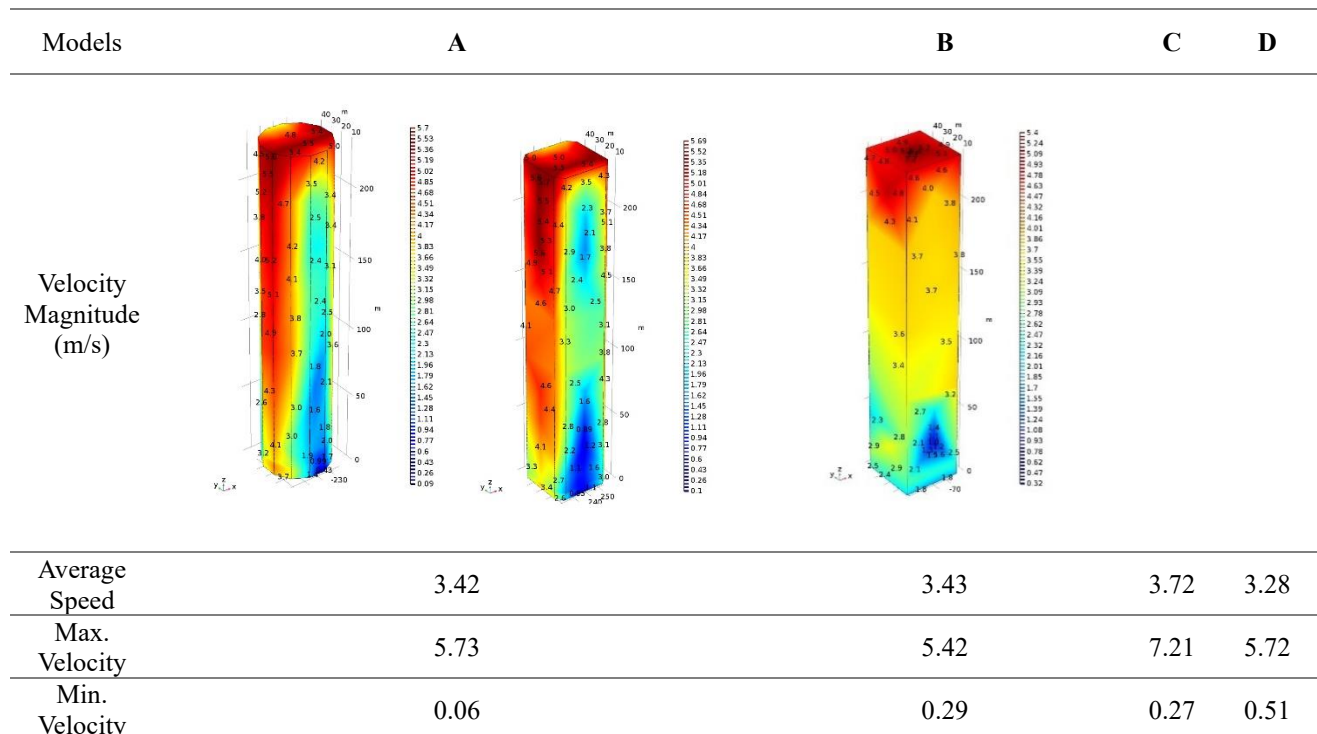


**Fig. 5: The Wind Tunnel Simulation Results**

To elucidate the characteristics of 2D turbulent flow around a square cylinder shape with modifications, the drag and lift coefficients, velocity vectors, and Strouhal number were plotted on different corner shapes. The velocity vectors around square cylinders with rounded, chamfered, and sharp corners are shown in Fig. 6. It should be noted that the separating flows from the windward edge of the square cylinder with corner modification commence to reattach to the cylinder surface. In addition, it is remarkable that the separation areas for the side faces of square cylinders with both rounded and chamfered corners are smaller than those of square cylinders with sharp corners.

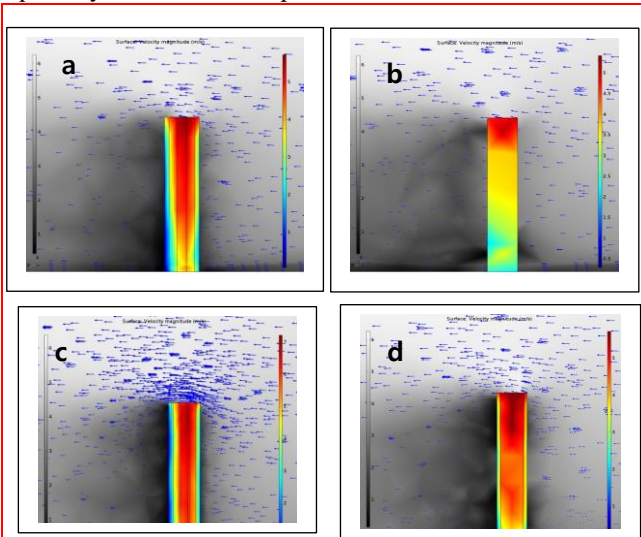


**Fig. 6: The Wind Action When Hitting the Buildings**

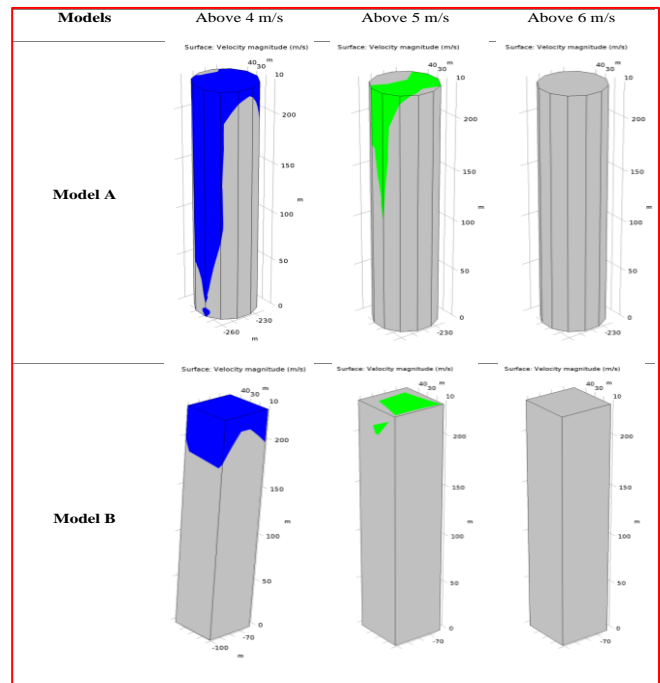
Looking at the XY cross-sections of the four models at the center of the COMSOL wind tunnel simulation, the magnitude of the velocity as a whole skyrocketed with altitude. As shown in Fig. 7, Model A reached its highest wind speed at 100 m above the ground and 125 m above the ground, which decreased slightly with height. This turbulence creates vertical coordinates in horizontally moving air at various levels, affecting the dispersion of pollutants, as well as dirt, sand, and soil particles in the air.

The slowdown near the surface is a function of the surface roughness. Wind speed profiles vary widely, depending on the type of terrain. In cities and rough terrains, the influence of wind gradients can reduce the land leaching speed by 40-50% above the air. In open water or ice, the reduction was likely to range from 20% to 30%.

Likewise, it may be inferred that the surface roughness does not affect Model B, and its impact vanishes slowly at higher elevations. In the examination with COMSOL, while wind blows from the southern front, wind ingestion is greater at the western and eastern fronts than at the south front. This reality directs the concentration toward another part of the wind energy, Table 3. Among all the models, Model B has the most honed corners, which can scarcely lead wind to other sides rather than to the south. This demonstrates that wind will generally be sped up by sharp corners without chamfered edges. Additionally, the roundabout design is productive in diminishing the parallel float of the structure and is successful in decreasing torsional loads. Owing to the roundabout shape in Model C, the wind blowing from the south is directed toward the east and west. The tallness of the structure does not affect the expanding wind speed in Model C, which can

be a negative point in planning energy-productive tall structures. Comparing Models, A and C, it is clear why chamfered and bent edges have better performance in wind energy absorption, which makes the structure a productive option for future models. The sudden rise in velocity in Model D, especially at an altitude of 175 m, shows that buildings with rectangular chamfered shapes outperform those with sharp corners in terms of wind absorption. It can be concluded that chamfered edges are the most fundamental factor in the increase in energy absorption, as the only difference between Models A and C is the curved edges. However, Model C was the only model that could not absorb wind energy on the roof, which is an interesting observation in this study. This suggests that circular shapes perform better on vertically rather than horizontally derived wind energy. At lower speeds, chamfered edges have a positive contribution to wind harvesting, which is clearly due to the alteration of wind direction shown in Models B and D.

**Table-3: The wind Velocity Above 4, 5, 6 m/s in Four Models**



#### IV. DISCUSSION

In this research, assessment of wind energy potential started with the analysis of climate data. In the next step, an understanding of the local climate was made on the basis of a detailed meteorological investigation. After the collection of required data, four possible arrangements of high-rise building were examined in relation to flow characteristics including terrain roughness and wind velocity. Given the first research question, whether shape can affect the characteristics of wind flow around tall buildings, it can be said that the simulation results showed that the concentration of wind load and the mean wind speed varied depending on the type of building shape.

## The Impact of High-Rise Building Shapes on Wind Flow Characteristics and Energy Potential

The investigation was followed by gathering aerodynamic information of the building and the site. The wind speed profile was used for showing the average wind speed distribution with height taking surface roughness into consideration.

These collected data were applied to CFD simulation as the inlet boundary condition for obtaining wind velocities at different altitudes above the ground. The results of CFD simulation and climate data were used in combination to assess wind speed conditions around the building. In the other hand, high-rise buildings showed considerable potential value to achieve sufficient wind speed for turbine installation. Addressing the second research question, whether there is a positive relationship between wind speed and energy potential that can be gained from the design of high-rise building, a sufficient wind speed was found for the design arrangement of wind turbines, positively correlated with the possible energy that could be harnessed from a humid tropical climate. The highest wind energy yield belonged to Model C with the most sufficient mean wind speed for vertical-axis wind turbines. This type of turbines can resist higher turbulences with a lower tip velocity and smaller noise effects and seem rather favoured for an urban wind energy development. The optimal wind penetration of Model C can be attributed to the efficiency of corner correction in circular plans. This finding shows that it is possible to provide better aerodynamic performance by carefully changing the shape of the corners. The experimental wind pressure measurements and analysis represented herein lead to identification of the influence of side ratio and wind orientations on wind pressure distribution and mean responses of the square/rectangular buildings. Wind pressure distribution on windward wall of rectangular models is almost independent of its side ratio at  $0^\circ$  wind incidence angle. Wind incidence angles and side ratio of buildings significantly affect the suction on side-walls and leeward wall of the buildings. As the side ratio approaches to about 3.0, the final steady reattachment of the flow takes place on side faces at  $0^\circ$  wind incidence angle. On the other hand, the negative pressure coefficient becomes almost constant as the side ratio exceeds 3.0, indicating that when depth is about three times the breadth, the lower limit of the wake width, which is approximately the full width of the body, is obtained. However, side ratio has little influence on the variation of wind pressures along the vertical direction. As the side ratio of building increases, the displacement of building along the X-axis decreases at  $0^\circ$  wind incidence angle due to the reduction of frontal area and increase in stiffness of building along the direction of forces. As the side ratio of building increases, the displacement of building along the Z-axis increases at wind incidence angle of  $90^\circ$  due to increase in the frontal area and reduction in stiffness along the direction of forces. As the side ratio of building increases, the torque developed due to uneven mean pressure distribution around the building walls also increases. The eccentricity between resultant wind force and centre of stiffness (and also the torque) is larger when the wind is nearly parallel to the long axis, than when it is nearly parallel to the short axis. The rapid rate of change in the mean torque around  $h = 0^\circ$  is thus principally due to the shift of the centre of pressure of side face-B toward leading corner. The third research question, whether aerodynamic changes in the corners of high-rise buildings are related to the wind characteristics, can be thus replied in such a way that the average of wind speed varied from one tower to another according to their aerodynamic

changes, but it was maximized on the roof of Tower C. This result is consistent with the results of Tamura and Elshaer et al [10,12][29] who claimed that simulation of wind loads and basic flow statistics can predict the aerodynamic improvements in the design of building. In order to design the buildings for Performance Level (PL), one way is using the energy absorption techniques, so that the main structural elements remain almost intact, or at least, easily repairable. In this regard, different researchers have proposed several methods so far. Tsai [12][30] has performed the research on TPEA device as seismic damper for high-rise buildings. Also, Shiba and his colleagues [13] have discussed control systems for tall buildings. Zhou has worked on the use of high-efficiency energy absorbing device to arrest progressive collapse of tall building [14].

There was a significant difference in the maximum velocity of wind between Models A and B as well as Models C and D especially at higher altitudes. In line with the claim of Bogle [15], focusing on the wind speed at high altitudes is a key design factor, which can significantly improve the potential operational output of wind turbines. The simulation results showed that towers with circular shapes had better performance than those with rectangular shapes on wind energy absorption. This is a positive answer to the fourth research question, whether the circular tower plans outperform the rectangular ones in energy exploitation for wind turbine installation. In a similar way, Sari and Cho [16] concluded that higher velocities and lower turbulences lead to greater wind energy potentials. Their CFD simulation results showed that round roof buildings compared to square roof buildings could enhance wind velocity by as much as 30%. In response to the fifth research question, whether chamfered and softened edges are promising in high-rise building design of the tropics, pairwise comparisons were made. As shown by the study findings, maximum wind velocity was higher for Model C than Model A as well as Model D than Model B. The wind concentration was also higher around Models C and D than Models A and B. These findings can be attributed to the effective role of corner modification in harvesting wind at lower speeds of a humid tropical urban area for generating electricity. According to the results of this study, the alternation of wind direction in Model C and Model D had a positive contribution to wind harvest and this is clearly due to their chamfered and softened edges. Similar result was obtained by Sari and Cho [16] who reported a 34% increase in wind velocity at round corners compared to sharp corners of a high tower. This result supports the outcome of fundamental studies mostly conducted on aerodynamic improvement by corner modification [10,17-24], each resulted in a way in the effectiveness of chamfering and rounding of corners for energy simulation in building design. Whereas Elshaer et al. [11][28] achieved sufficient accuracy for 2D models in reducing lift (across-wind) and drag (along-wind) forces followed by chamfered and rounded edges, Tamura [25] reported 10% decrease in lift and drag coefficients for 3D compared to 2D turbulent model simulation.

## V. CONCLUSIONS

The results of the current study investigated that a flat geometry with a small number of straw breaks is a beneficial parameter and if chosen properly can provide significant benefits. Furthermore, the rounded square building is the most effective in suppressing the aeroelastic instability and the amplitude of wind-induced vibrations decreases as the degree of rounded corners increases. The data indicated that the taper effect was more significant across than along the wind direction, and depending on the wind direction and crosswind direction, through-holes, especially in the upper part of the building, reduce the wind excitation by the building.

## ACKNOWLEDGMENTS

The research described in this paper was financially supported by the Universiti Putra Malaysia

## DECLARATION STATEMENT

Funding	No, I did not receive.
Conflicts of Interest	No conflicts of interest to the best of our knowledge.
Ethical Approval and Consent to Participate	No, the article does not require ethical approval and consent to participate with evidence.
Availability of Data and Material	Not relevant.
Authors Contributions	All authors have equal participation in this article.

## REFERENCES

- Elshaer, A., Gairola, A., Adamek, K., & Bitsuamlak, G., "Variations in wind load on tall buildings due to urban development", *Sustainable cities and society*, 34(2017) 264-277. <https://doi.org/10.1016/j.scs.2017.06.008>
- Walker, S. L., "Building mounted wind turbines and their suitability for the urban scale—A review of methods of estimating urban wind resource", *Energy and Buildings*, 43(8)(2011), 1852-1862. <https://doi.org/10.1016/j.enbuild.2011.03.032>
- Hassanli, S., Hu, G., Kwok, K. C., & Fletcher, D. F., "Utilizing cavity flow within double skin façade for wind energy harvesting in buildings", *Journal of Wind Engineering and Industrial Aerodynamics*, 167(2017) 114-127. <https://doi.org/10.1016/j.jweia.2017.04.019>
- Trikootam, S. C., & Hornikx, M., "The wind effect on sound propagation over urban areas: Experimental approach with an uncontrolled sound source", *Building and Environment*, 149(2019) 561-570. <https://doi.org/10.1016/j.buildenv.2018.11.037>
- Versteeg, H. K., & Malalasekera, W., "An introduction to computational fluid dynamics", the finite volume method. Pearson prentice hall publication. (2nd edition).(2007)128-137. <https://doi.org/10.1098/rsta.1895.0004>
- Reynolds, O., "IV. On the dynamical theory of incompressible viscous fluids and the determination of the criterion", *Philosophical transactions of the royal society of london.(a.)*, (186)(1895) 123-164.
- Gimenez, J. M., & Bre, F., "Optimization of RANS turbulence models using genetic algorithms to improve the prediction of wind pressure coefficients on low-rise buildings", *Journal of Wind Engineering and Industrial Aerodynamics*, 193(2019) 103978. <https://doi.org/10.1016/j.jweia.2019.103978>
- Fredsoe, J., "Turbulent boundary layer in wave-current motion", *Journal of Hydraulic Engineering*, 110(8)(1984), 1103-1120. [https://doi.org/10.1061/\(ASCE\)0733-9429\(1984\)110:8\(1103\)](https://doi.org/10.1061/(ASCE)0733-9429(1984)110:8(1103))
- Klostermeyer, J., "Parametric instabilities of internal gravity waves in Boussinesq fluids with large Reynolds numbers", *Geophysical & Astrophysical Fluid Dynamics*, 26(1-2)(1983), 85-105. <https://doi.org/10.1080/03091928308221764>
- Tamura, T., & Miyagi, T., "The effect of turbulence on aerodynamic forces on a square cylinder with various corner shapes", *Journal of Wind Engineering and Industrial Aerodynamics*, 83(1-3)(1999), 135-145. [https://doi.org/10.1016/S0167-6105\(99\)00067-7](https://doi.org/10.1016/S0167-6105(99)00067-7)
- Elshaer, A., Aboshosha, H., Bitsuamlak, G., El Damatty, A., & Dagnev, A (2016), "LES evaluation of wind-induced responses for an isolated and a surrounded tall building", *Engineering Structures*, 115(2016) 179-195. <https://doi.org/10.1016/j.engstruct.2016.02.026>
- Tsai, C. S., & Tsai, K. C., "TPEA device as seismic damper for high-rise buildings", *Journal of engineering mechanics*, 121(10)(1995)1075-1081. [https://doi.org/10.1061/\(ASCE\)0733-9399\(1995\)121:10\(1075\)](https://doi.org/10.1061/(ASCE)0733-9399(1995)121:10(1075))
- Shiba, K., Mase, S., Yabe, Y., & Tamura, K (1998), "Active/passive vibration control systems for tall buildings", *Smart materials and structures*, 7(5)(1998)588. <https://doi.org/10.1088/0964-1726/7/5/003>
- Zhou, Q., & Yu, T. X., "Use of high-efficiency energy absorbing device to arrest progressive collapse of tall building", *Journal of Engineering Mechanics*, 130(10)(2004)1177-1187. [https://doi.org/10.1061/\(ASCE\)0733-9399\(2004\)130:10\(1177\)](https://doi.org/10.1061/(ASCE)0733-9399(2004)130:10(1177))
- Bogle, I., "Integrating wind turbines in tall buildings", *CTUH Journal*, 4(2011) 30-33.
- Sari, D. P., & Cho, K. P., "Performance Comparison of Different Building Shapes Using a Wind Tunnel and a Computational Model", *Buildings*, 12(2)(2022), 144. <https://doi.org/10.3390/buildings12020144>
- Kwok, K. C., & Bailey, P. A., "Aerodynamic devices for tall buildings and structures", *Journal of engineering mechanics*, 113(3)(1987)349-365. [https://doi.org/10.1061/\(ASCE\)0733-9399\(1987\)113:3\(349\)](https://doi.org/10.1061/(ASCE)0733-9399(1987)113:3(349))
- Kawai, H., "Effect of corner modifications on aeroelastic instabilities of tall buildings", *Journal of wind engineering and industrial aerodynamics*, 74(1998) 719-729. [https://doi.org/10.1016/S0167-6105\(98\)00065-8](https://doi.org/10.1016/S0167-6105(98)00065-8)
- Gu, M., & Quan, Y., "Across-wind loads of typical tall buildings. *Journal of Wind Engineering and Industrial Aerodynamics*, 92(13)(2004) 1147-1165. <https://doi.org/10.1016/j.jweia.2004.06.004>
- Tse, K. T., Hitchcock, P. A., Kwok, K. C., Thepmongkorn, S., & Chan, C. M., "Economic perspectives of aerodynamic treatments of square tall buildings", *Journal of Wind Engineering and Industrial Aerodynamics*, 97(9-10)(2009), 455-467. <https://doi.org/10.1016/j.jweia.2009.07.005>
- Tanaka, H., Tamura, Y., Ohtake, K., Nakai, M., & Kim, Y. C., "Experimental investigation of aerodynamic forces and wind pressures acting on tall buildings with various unconventional configurations", *Journal of Wind Engineering and Industrial Aerodynamics*, 107(2012) 179-191. <https://doi.org/10.1016/j.jweia.2012.04.014>
- Carassale, L., Freda, A., & Marre-Brunenghi, M., "Experimental investigation on the aerodynamic behavior of square cylinders with rounded corners. *Journal of Fluids and Structures*", the Seventh International Colloquium on Bluff Body Aerodynamics and Applications (BBAA7) Shanghai, China; September 2-6, 2012. 44(2014) 195-204. <https://doi.org/10.1016/j.jfluidstructs.2013.10.010>
- Xie, J., "Aerodynamic optimization of super-tall buildings and its effectiveness assessment", *Journal of Wind Engineering and Industrial Aerodynamics*, 130(2014) 88-98. <https://doi.org/10.1016/j.jweia.2014.04.004>
- Elshaer, A., Bitsuamlak, G., & El Damatty, A., "Aerodynamic shape optimization for corners of tall buildings using CFD", In 14th international conference on wind engineering (ICWE).(2015). [https://doi.org/10.1016/S0167-6105\(98\)00048-8](https://doi.org/10.1016/S0167-6105(98)00048-8)
- Tamura, T. E. T. S. U. R. O., Miyagi, T., & Kitagishi, T "Numerical prediction of unsteady pressures on a square cylinder with various corner shapes", *Journal of Wind Engineering and Industrial Aerodynamics*, 74(1998) 531-542. <https://doi.org/10.35940/ijeat.D9016.049420>
- Jagtap, R. D., Singh, D. P., Singh, E., Shinde, P., & Dixit, A. (2020). Technological Intervention for Effective Strategies Formulation and Implementation. In *International Journal of Engineering and Advanced Technology* (Vol. 9, Issue 4, pp. 1943–1951). <https://doi.org/10.35940/ijeat.d9016.049420>
- Malik, S., & Sharma, P. (2019). Performance Evaluation of Automated System over Manual System of PPM in Urban Development. In *International Journal of Innovative Technology and Exploring Engineering* (Vol. 8, Issue 11, pp. 2048–2050). <https://doi.org/10.35940/ijitee.k1931.0981119>

28. Adhikari, B., & Poudel, A. (2023). Comparative Study of Building Response on Adoption of NBC105: 2020 and IS 1893 (Part 1): 2016. In *Indian Journal of Structure Engineering* (Vol. 3, Issue 1, pp. 14–21). <https://doi.org/10.54105/ijse.c4006.053123>
29. Adha Misman, M. R., Azmi, A. M., Kamarul Baharin, Z. A., & Abdul Hamid, A. H. (2019). The Effect of Slat Opening on Vortex Shedding Behind a Circular Cylinder. In *International Journal of Recent Technology and Engineering (IJRTE)* (Vol. 8, Issue 4, pp. 6879–6885). <https://doi.org/10.35940/ijrte.d5210.118419>.
30. Mustafa, S., & Mustafa, A. (2023). Influence of Soils Conditions on the Macroseismic Effects in the Dukagjin Area Based the Seismic Wave Propagation from Durres Earthquake 26/11/2019. In *International Journal of Basic Sciences and Applied Computing* (Vol. 10, Issue 2, pp. 9–16). <https://doi.org/10.35940/ijbsac.b0508.1010223>

## AUTHORS PROFILE



**Ehsan Mokhtari**, He is originally from Mashhad-Iran. He studied BSc in the field of engineering in Iran. He got his BSc from Iran then he came to Malaysia to complete his study. He graduated (Master of Science) from Department of Design and Architecture, Faculty of Design and Architecture, Universiti Putra Malaysia-UPM in 2022. His interest is on Civil Engineering, Acoustic Engineering and

Architectural Engineering. During his study and research, Sustainable Construction, Construction and Energy Efficiency in Building were the main skills and experiences that he acquired. The impact of high-rise building shapes on wind flow characteristics and energy potential was the first paper that he worked on it. He is trying to continue this project and improve it for his next project.



**Amir Hossein Jafari**, He is originally from Iran. Amirhossein is the 3rd child in his family. His father was also civil engineer and he tried to learn more from his father. In many project he helped his father and designed many building based on new technology. He studied in civil engineering at Islamic Azad University-Lahijan Branch. His diploma was on building structure and designing. He is working as an editor on

manuscripts that are related to his filed. He likes civil engineering and trying to do more project in this filed. In the current project, he edited the manuscript. He is trying to do the same project in high-rise building shapes in Iran.



**Roslina Sharif**, she got her PhD (Architecture), from Universiti Teknologi in Malaysia. Her MSc was in the field of Instructional Technology from University of Malaya. She got BSc in Environmental Design/Architecture from Texas A&M University, Texas USA. Currently, she is working as a senior lecturer at university Putra Malaysia and research on

Architecture/Environmental Design. Sofar she has 46 citations with 4 h-index. She is trying to work more the same project in Malaysia. She edited and wrote articles, conference papers, journals and book chapters in STEdex, PAX publications and the 'Thinking Hands of Hajeedar' book. She peer-reviewed articles in conferences and academic journals such as the Journal of Built Environment (UKM), and Pertanika Journal of Social Sciences and Humanities.



**Wan Srihani**, PhD in Architecture from University of Malaya, Malaysia. She got MA in Urban Design from Oxford Brookes University, UK. Her Post Graduate Diploma was in Architecture from Oxford Brookes University, UK. Currently, she is working at Department of Architecture, Faculty of Design & Architecture, UPM

Malaysia. Self Help Housing, Affordable Housing, Low Technology Construction are Field of her Specialization. From 2014 to 2016, Wan Srihani led the team of more than 150 staff and volunteers in completing 25 houses for the Orang Asli community. She envisions the program as a manifestation of the principles of responsible architecture, offering a new rapid-construction approach to enable low-income groups to build affordable and scalable homes using locally-sourced materials, at the same time retaining their traditional architecture styles

**Disclaimer/Publisher's Note:** The statements, opinions and data contained in all publications are solely those of the individual author(s) and contributor(s) and not of the Lattice Science Publication (LSP)/ journal and/ or the editor(s). The Lattice Science Publication (LSP)/ journal and/or the editor(s) disclaim responsibility for any injury to people or property resulting from any ideas, methods, instructions or products referred to in the content.